JMEPEG (2006) 15:376-382
DOI: 10.1361/105994906X113705

1059-9495/$19.00

Plasma Synthesis of Carbon-Iron Magnetic Nanoparticles and Immobilization of Doxorubicin for Targeted Drug Delivery

Y. Ma, S. Manolache, F. Denes, D. Vail, D. Thamm, and I. Kurzman

(Submitted December 9, 2005; in revised form April 24, 2006)

A novel dense-medium plasma technology (submerged arc discharge) was used to synthesize carbon/iron-based magnetic nanoparticles (CMNP) from benzene or acetonitrile at room temperature and atmospheric pressure. Scanning electron microscopy shows that the nanoparticles are spherical and 40-50 nm in diameter. Results from x-ray photoelectron spectroscopy and other analytical techniques demonstrated that the CMNP consist of iron/iron oxide clusters that are evenly dispersed in a carbon-based host-structure. After synthesis, CMNP samples were activated in three steps: argon plasma treatment, in-situ reactions with ethylene diamine, and substrate activation by glutaric dialdehyde. Free doxorubicin (DOX) molecules were then immobilized onto the activated CMNP surfaces to form CMNP-DOX conjugates. The loading efficiency of doxorubicin was determined. In vitro anti-proliferative activity of CMNP-DOX conjugates was confirmed in tumor-cell cytotoxicity assays. It is therefore suggested that CMNP may be used as a magnetic carrier for targeted drug-delivery applications.

Keywords: doxorubicin, immobilization, magnetic nanoparticles, plasma, targeted drug delivery

1. Introduction

In cancer treatment, chemotherapy can be very effective against the deadly illness but often carries with it severe side effects due to the high levels of toxins used to destroy malignant or virulent cells but which also kill healthy cells. Therefore, people have been trying for many years to find better ways to fight cancers. One potential solutions is targeted drug delivery, i.e., using a certain vehicle to deliver a selected amount of anticancer agent directly to the tumor for localized cancer treatment. This on-target delivery should dramatically decrease side effects, improve drug efficiency, and reduce required dosages.

In the world of nanotechnology, as many as 250 billion nanoparticles could fit snugly in the period at the end of this sentence. Being so small, these particles have many very unique chemical and physical properties, such as lower melting points, increased light absorption, and different electromagnetic properties, which make them important players in a host of applications. Some researchers believe that nanosized particles even constitute another state of matter.

Among the various new properties of nanomaterials, magnetism is of special interest in solving the aforementioned problem of nonspecific cancer-chemotherapy toxicity. Magnetic nanoparticles embedded in nonmagnetic host materials, including carbon structures, polymers, and dielectric oxides, provide encapsulation and prevent both grain growth and agglomeration. Combination of magnetic and dielectric characteristics can result in multifunctionalities with potential applications in advanced technologies, such as development of miniature and efficient data-storage devices, novel and efficient targeted cancer drug delivery systems, replacement of radioactive tracer materials by high-quality noninvasive medical imaging, and adsorption followed by removal of radioactive metals from toxic waste materials by strongly magnetic nanoparticle systems (Ref 1-7).

More importantly, by application of an external magnetic field, cancer drugs that have been attached to nanoparticles may be directed to the local tumor site, thus maximizing drug exposure to tumor tissues and minimizing exposure to normal tissues. Due to their high intrinsic magnetic moment, the iron-based paramagnetic nanoparticles are particularly important and promising for this type of targeted drug delivery. This allows good magnetic guidance inside biological systems while retaining no magnetic remanence (residual magnetism). Compared with other delivery methods, such as liposomes and antibodies, tiny magnetic nanoparticle carriers can offer several advantages: liposomes are particles large enough to be captured by macrophages, and antibodies are inefficient to distinguish normal cells from tumor cells, whereas nanoparticles may avoid the liver and spleen and reach the target tissues because of their small size. In addition, the linkages between the nanoparticle carriers and cancer drugs can be designed in such a way that the drug-release profile may be controlled for when and where to release the drug (Ref 8-10).

Currently, several different iron-based paramagnetic nanoparticle drug-delivery systems have been reported (Ref 11-14). Although the particular procedures to produce the magnetic nanoparticles are different, they usually do have something in

This paper was presented at the Third International Surface Engineering Congress and Exposition held August 2-4, 2004 in Orlando, FL.

Y. Ma, S. Manolache, and **F. Denes,** Center for Plasma-Aided Manufacturing, University of Wisconsin, Madison, WI 53706; **D. Vail, D. Thamm,** and **I. Kurzman,** School of Veterinary Medicine, University of Wisconsin, Madison, WI 53706. Contact e-mail: denes@engr.wisc.edu.

common: iron oxide nanoparticles (Fe_3O_4 and/or Fe_2O_3) were either prepared in the laboratory or purchased from other sources, and then a variety of molecules (e.g., alcohol, dextran, albumin, organosilanes, and methacrylates) were coated onto the iron nanoparticles through polymerization. Nanoparticles formed in this way are essentially a metal core that is incorporated in a polymer matrix, and the iron oxides are not evenly distributed throughout the matrix. Resulting nanoparticle diameters range from 10 to 100 nm.

In this paper, a patented dense-medium plasma (DMP) technology will be used that allows initiation and sustainment of discharges in a co-existing liquid/vapor medium at atmospheric pressure and offers a significantly higher efficiency for the processing of liquid-phase materials in comparison to other existing plasma technologies. Carbon-based magnetic nanoparticles (CMNP) were synthesized from an arc sustained in either benzene or acetonitrile between iron electrodes. The DMP-synthesized nanoparticle system is composed predominantly of a carbon-based host structure in which the iron and iron oxide particles are evenly dispersed. The CMNP were then plasma-functionalized and activated, and doxorubicin was subsequently immobilized onto their surfaces. Reactivity of the immobilized drug was evaluated.

2. Materials and Methods

2.1 Materials and Characterization Techniques

Benzene and acetonitrile (99%) used as precursors of the CMNP was purchased from Aldrich Co. (St. Louis, MO) Argon was purchased from Liquid Carbonic Industries Corp. (Danbury, CT), and was used as cavitation-generating inert gas during the synthesis and as plasma gas during the surface functionalizations. Ethylene diamine (ED, 99%, bp 118 °C) and glutaric dialdehyde (GD, 25 wt.% solution in water, bp 101 °C) used for immobilization were also purchased from Aldrich Co. Fluorescamine used for the identification of primary amine functionalities was purchased from Molecular Probes, Inc. (Eugene, OR). Doxorubicin hydrochloride (DOX, ≥95%) was purchased from Fisher Scientific (Hampton, NH).

Electron spectroscopy for chemical analysis (ESCA), also known as x-ray photoelectron spectroscopy (XPS), was used for evaluation of relative surface atomic concentration and C1*s* surface functionalities of the CMNP and the CMNP-DOX conjugates. The instrument and the corresponding parameters that were used are a Perkin-Elmer Physical Electronics Phi5400 small-area ESCA system; Mg source, 15 kV, 300 W; pass energy, 89.45 eV; take-off angle, 45°. Samples were mounted onto the holder with double-sided copper tapes to reduce sample charging, and they were usually pumped for 2 h in the prechamber for degassing before being introduced into the main chamber.

Scanning electron microscope (SEM) images were collected using a LEO 1530 field-emission SEM (LEO Electron Microscopy, Inc., Thornwood, NY). Samples were mounted using a piece of double-sided copper tape and were coated with gold by sputter deposition. The sputtering device was a Denton Vacuum Inc. (Moorestown, NJ) Desk II system; the pressure of sputtering gas (argon) was 50 mtorr, the sputtering current was 45 mA, and the sputtering time was 10 s.

An Ultima ICP-AES inductively coupled plasma mass spectrometry (ICP-MS) instrument (Jobin-Yvon, Edison, NJ) was used. Samples were wet-ashed and extracted with nitric acid and hydrogen peroxide at 140 °C and 100 psi for 25 min. They were then filtered into volumetric flasks, and elemental analyses were carried out.

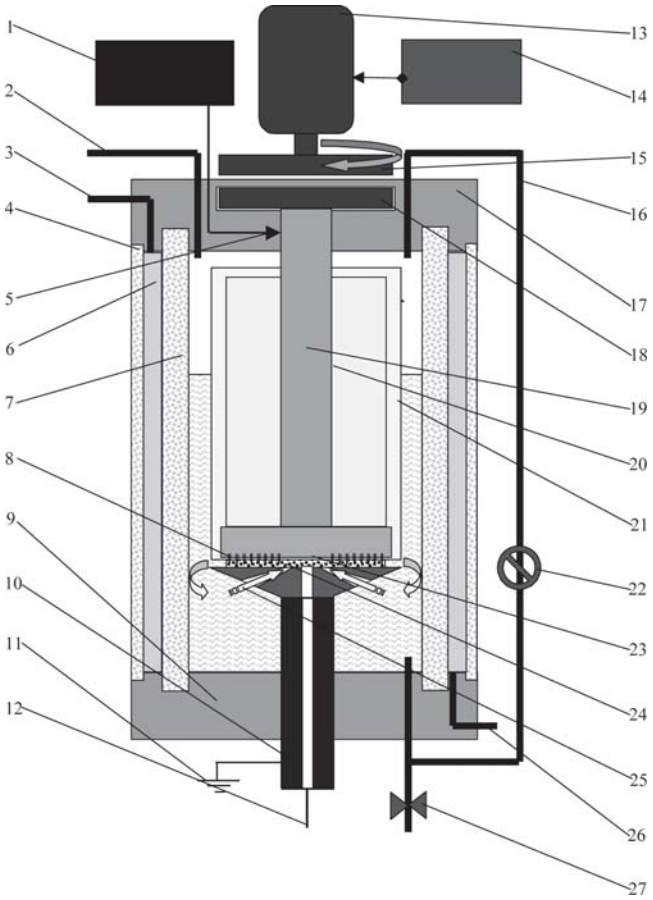

Fig. 1 Redesigned DMP reactor: (1) DC power supply; (2) gas evacuation point; (3, 26) coolant exit and inlet; (4, 7) glass cylinders; (5) electrical contact; (6) coolant; (8) ceramic-pin array; (9, 17) caps; (10) non-rotating electrode; (11) ground; (12) gas inlet; (13) motor; (14) digital controller; (15, 18) magnetic coupling system; (16) liquid inlet; (19) rotating electrode; (20) sealed volume; (21) quartz isolator; (22) recirculating pump; (23) pins; (24) electrical discharges; (25) recirculated flux; (27) valve

2.2 Plasma Synthesis of CMNP

The plasma synthesis of CMNP from benzene was performed using an original DMP reactor, which was designed and developed at the Center for Plasma-Aided Manufacturing, University of Wisconsin-Madison (Ref 15-17). The DMP reactor allows the initiation and sustainment of discharges at atmospheric pressure environments, in co-existing liquid/vapor medium and may offer a significantly higher efficiency for the processing of liquid-phase materials in comparison to existent plasma technologies.

Figure 1 shows the design of this DMP reactor. It is basically composed of a vacuum-tight cylindrical glass chamber where liquid medium to be treated is contained. A set of electrodes is immersed within the liquid medium. The upper electrode has a ceramic disc cap, on top of which is located an array of metal pins. The lower electrode is a metal disc with three

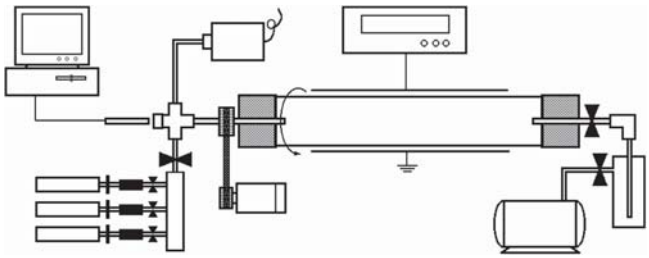

Fig. 2 Schematic diagram of the radio frequency rotating plasma reactor system used for surface functionalization of CMNP (Ref 19)

holes for the purpose of facilitating liquid circulation. Both electrodes can be made from certain metals as required for the particular treatment. The distance between the electrodes can also be adjusted as desired.

For plasma treatment, the upper electrode can be rotated at high speed (up to 5,000 rpm) whereas the lower electrode is stationary. Inert or reactive plasma gas is bubbled through the liquid medium from the bottom of the glass chamber. A combination of these two motions generates many microcavities between the electrodes. At this time, the direct current (dc) power supply is turned on and plasma is initiated within the many microcavities. Active species (e.g., free radicals) diffuse toward the interface and react with liquid medium. Rotating the electrode also helps homogenize the microdischarges, activate a larger effective volume of fluid, pump fresh liquid medium into the discharge zone, and decrease the boundary layers between the emission tips and the bulk liquid. More detailed descriptions of the DMP reactor can be found in previous publications (Ref 15-18).

During a typical process to synthesize the CMNP nanoparticles, 200 mL of benzene or acetonitrile is introduced into the DMP reactor and argon is injected through the hollow, lower electrode at the selected flow rate. The cooling of the reaction medium is started by tap water flowing through the cooling jacket, and the rotation of the upper electrode is started at the desired angular speed. The discharge is initiated, and the plasma state is sustained for the selected treatment time. The following experimental conditions were used during the synthesis: type of electrode, iron; dc voltage, 200 V; current, 1 A; angular speed of the rotating electrode, 1,000 rpm; plasma gas, argon; flow rate of argon, 3 sccm; temperature of the reaction media, 18 °C; treatment time, 3 min.

The resulting CMNP suspension was separated by using 30 mL Teflon centrifuge tubes and a Fischer Scientific Marathon 22K centrifuge at 3,000 rpm and for 15 min. The supernatant was then removed with the help of a pipette, and the remaining carbon particles were mixed with 25 mL of fresh benzene/acetonitrile, stirred, and then centrifuged again, to wash away soluble byproducts that resulted from the DMP treatment. This washing process was repeated 4-6 times until the supernatant turned from brown-yellow to colorless. The resulting carbon nanoparticles were dried in a vacuum oven at 50 °C for at least 24 h.

2.3 Surface Functionalization of CMNP

Figure 2 shows the reactor that was used to surface functionalize the CMNP for the subsequent immobilization reactions. It is a capacitively coupled, 13.56 MHz RF rotating plasma installation. Compared with other typical plasma systems, such as parallel-plate reactors, this rotating reactor is capable of surface treatment of powdery substrates. Due to the rotation of the glass reactor chamber, fresh surfaces of the powdery samples can be constantly brought out for plasma exposure, leading to uniform surface functionalization (Ref 19).

In a typical experiment, the untreated, vacuum-oven-dried CMNP were loaded into the reactor chamber, which had been cleaned previously using oxygen plasma at 100 W for 10 min to remove any contamination from previous runs. By operating the flow controllers and the corresponding needle valves, the required argon pressure and flow rate were achieved in the reactor. The rotation of the reactor was then started, and the plasma was ignited and sustained for the selected reaction time. At the end of the plasma exposure, the gas-feed valves were closed and the system was evacuated to the base pressure. With the vacuum line closed, ED vapor was then introduced in situ and the pressure inside the chamber was kept at 1 torr for 30 min, after which the vacuum line was opened and the system was pumped down for 30-40 min to remove adsorbed ED and/or other byproducts resulting from the treatment. The experimental parameters used during the plasma treatment are as follows: substrate, CMNP, 400 mg; plasma gas, argon; base pressure, 60-70 mtorr; Ar pressure in the absence of plasma, 200 mtorr; RF power dissipated into the chamber, 200 W (continuous); treatment time, 10 min.

2.4 Immobilization of Doxorubicin

In a slightly alkaline environment, aldehydes and ketones can react with primary and secondary amino groups to form Schiff bases. This reaction has been used by many researchers for coupling ligands, spacers, or proteins to certain supports (Ref 20, 21). Thus the following immobilization procedure was developed to bind free doxorubicin molecules onto the surfaces of functionalized CMNP particles.

Prior to immobilization, the CMNP substrate was washed with 50 mL of deionized water (twice) and 50 mL of 0.1 M pH 7 phosphate buffer. A 2% (weight) solution of GD was prepared by diluting 4 mL of 25% GD solution to 25 mL by using 0.1 M pH 7 phosphate buffer. Approximately 100 mg of CMNP substrate and 50 mL of the 2% GD solution were added together into a 50 mL beaker, which was then placed into a water bath (controlled by a Fisher Scientific Model 3210 Refrigerated Circulator) and incubated for 2 h at 40 °C. During the incubation, the CMNP/GD mixture was constantly mixed with a magnetic stirrer. The GD-coated CMNP substrates were then washed with 50 mL of 0.1 M pH 7 phosphate buffer, filtered, dried, and weighed with a Sartorius BA110S Basic series analytical balance (0.1 mg readability) to determine the amount of CMNP substrate left for subsequent immobilization.

Free doxorubicin hydrochloride (10 mg) was dissolved into 8 mL of 0.1 M pH 8 phosphate buffer to form a 1.25 mg/mL solution. The GD-coated CMNP samples were added into this solution and incubated in a 37 °C water bath for 3-4 h. The combination was then mixed with a magnetic stirrer during incubation. After this immobilization reaction, the CMNP-DOX conjugates were washed as follows to remove unreacted free doxorubicin molecules: (1) 0.1 M phosphate buffer (pH = 8), 50 mL; (2) deionized water, 25 mL; (3) 0.15 M NaCl solution, 25 mL; and (4) deionized water, 50 mL. At the end,

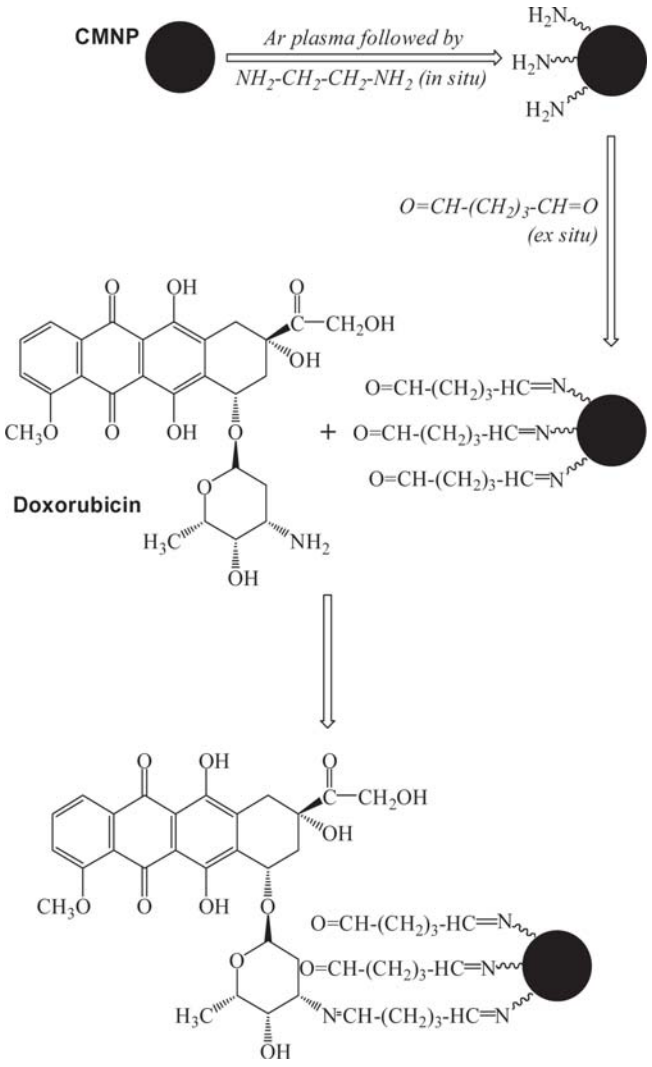

Fig. 3 Complete reactions to immobilize free doxorubicin onto the surfaces of carbon-based magnetic nanoparticles

the conjugates were filtered, dried in a vacuum oven at 50 °C, and stored for future analyses.

To determine how much doxorubicin was immobilized onto the CMNP substrate, the liquid left over from washing the CMNP-DOX conjugates in the previous step was collected, and it contained all of the unreacted drug molecules. Spectrophotometry (S1000 fiber optic spectrometer by Ocean Optics, Inc.) was used to measure this very low concentration of doxorubicin, so that it could be used to calculate the amount of drugs within the conjugates. A series of doxorubicin solutions were prepared, ranging from 7.8×10^{-4} to 5×10^{-2} mg/mL. The absorption was measured by the spectrophotometer over the range from 150 to 750 nm. The peak values at 460 nm were plotted against the doxorubicin concentration to obtain a calibration curve. After the absorption of the liquid left over after sample washing was measured, its corresponding doxorubicin concentration was determined with the help of this calibration curve.

Figure 3 shows all of the reactions that were mentioned above, including plasma surface functionalization of CMNP, generation of ketone groups on the nanoparticle substrate, and reaction between doxorubicin and CMNP particles.

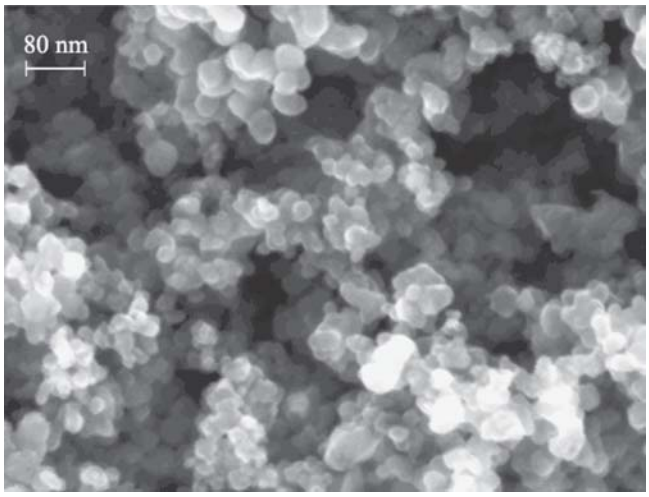

Fig. 4 SEM image of the carbon-based magnetic nanoparticles (original magnification 100,000×)

2.5 Activity Analysis

D17 canine osteosarcoma cells were obtained from ATCC (Manassas, VA) and were serially passaged by trypsinization in plastic tissue culture flasks in complete minimal essential medium (Gibco Invitrogen, Carlsbad, CA) containing 10% fetal bovine serum (C/10).

The in vitro anti-proliferative effect of CMNP-DOX on D17 cells was assessed utilizing a tetrazolium-based assay (MTS tetrazolium salt, CellTiter Aqeous One, Promega, Madison, WI). 3000 D17 cells per well were plated in 96-well plates in C/10 and incubated under standard conditions (37 °C, 5% CO_2, humidified); 24 h later, the plates were washed twice with Hanks' balanced salt solution, and the medium replaced with C/10 containing various concentrations of DOX (Bedford Laboratories, Bedford, OH) or equivalent concentrations of DOX conjugated to CMNP. A concentration of unconjugated CMNP equivalent to the highest concentration of CMNP-DOX used was included as a control. Each condition was assayed in quintuplicate. The plates were incubated for a further 72 h. Relative viable cell number was then assessed by adding 40 μL of MTS reagent to each well, incubating an additional 1-4 h, and then determining the absorbance of each well at 490 nm using a microplate absorbance spectrophotometer. Growth inhibition was expressed as a percentage, compared with cells incubated in C/10 alone (Ref 22, 23).

3. Results and Discussion

3.1 Characterizations of CMNP

Figure 4 is the SEM image of the carbon-based magnetic nanoparticles. The image shows that CMNP particles are composed of very uniform, spherical particles with diameters of 40-50 nm, which are small enough to escape detection by the body's immune system and easily pass through cell membranes but which are large enough to survive travel through the bloodstream to deliver the payload. Because magnetic properties of nanoparticles vary by size, the CMNP uniform size distribution ensures consistent properties of the carbon nanoparticles. It is also suggested that the liquid medium, where the solid-phase nanoparticles were generated due to the heterogeneous

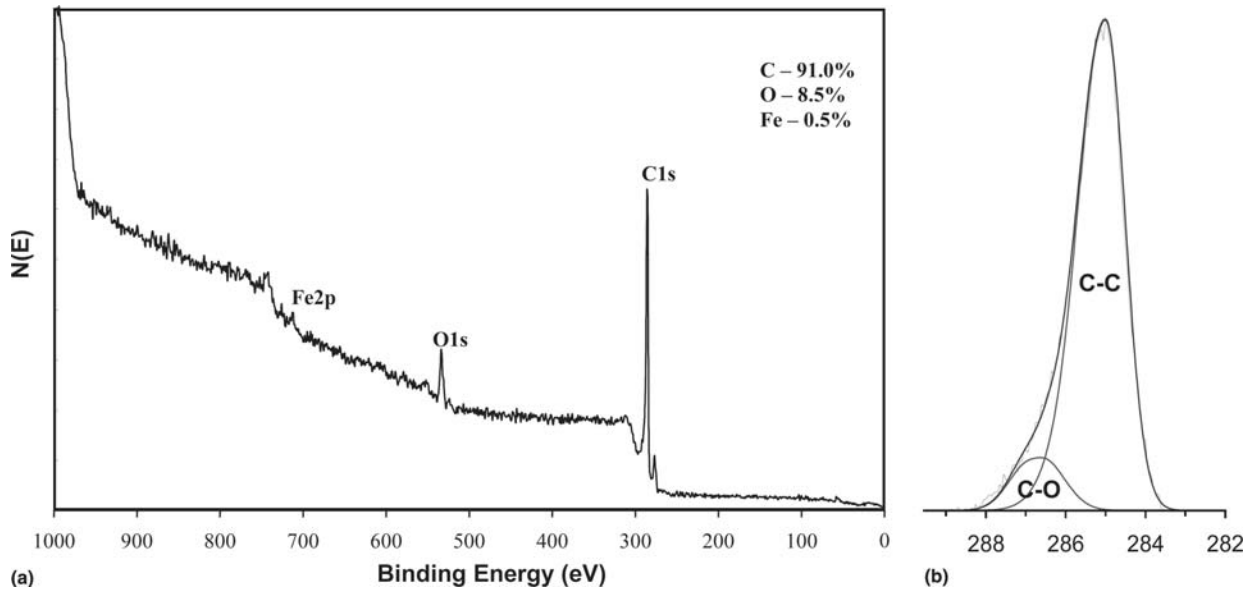

Fig. 5 (a) Survey of an ESCA spectrum and the surface atomic concentrations of the carbon-based C/Fe magnetic nanoparticles; (b) C1*s* high-resolution ESCA spectrum of the nanoparticles

interphase reactions, led to the formation of CMNP nanoparticles uniform in size and shape. We believe this heterogeneous medium synthesis route will open up additional efficient ways in the future for the generation of large quantities of pure and hybrid nanoparticle systems.

Survey ESCA data of the nanoparticles synthesized from benzene (Fig. 5a) indicate that the major component of the nanoparticles is carbon (91.0%). Oxygen and iron relative surface atomic concentrations are only 8.5% and 0.5%, respectively. The oxygen content of nanoparticles can be related to ex situ oxidation of the plasma-generated nanoparticles promoted by the discharge-created free radical sites and to the oxidation of iron particles caged into the carbon structure under open laboratory environments. The high-resolution (HR) ESCA diagram of nanoparticles (Fig. 5b) shows that C–C bonds with low binding energy (285.0 eV) account for 89.7% of the existing carbon atoms, suggesting that saturated C–C bonds are the dominant linkages of the nanoparticle structures. The rest of carbon atoms are connected to oxygen, forming C–O linkages (286.6 eV) that account for 10.3% of the entire C1*s* peak area. It can be calculated that the 10.3% C–O linkages correspond to an oxygen surface atomic concentration of 9.3%, which is almost same as what is obtained from ESCA survey results (8.5%). Therefore, it is safe to say that most of the oxygen atoms are connected to carbon atoms.

ESCA data of the acetonitrile-synthesized C/Fe/N nanoparticles are virtually identical to the data of benzene-originating C/Fe nanoparticles. The only difference is that C/Fe/N CMNPs contain a trace concentration of nitrogen (~1%) due to the acetonitrile used as the starting material.

Because of the low resolution of ESCA system, it is not suitable for measuring trace elements. Therefore, the iron concentration in the CMNP system was more precisely evaluated by ICP-MS, which shows Fe concentrations ranging from 0.8 to 1.2%.

These carbon-based C/Fe or C/Fe/N nanoparticles are magnetic. This was visually verified with the help of a neodymium supermagnet. It was observed that the magnet could easily move the carbon particles that were either contained in a glass vial or suspended in distilled water. Further analyses of the CMNP magnetic properties have been done through ferromagnetic resonance spectroscopy (FMR) and extended x-ray absorption fine structure spectroscopy (EXAFS) techniques. Detailed analyses have been presented in an earlier publication by Denes et al. (Ref 18) and are not included in this article due to space limitations. According to those published data, however, the C/Fe and C/Fe/N nanoparticles exhibit magnetic properties, and this behavior has been related to the presence of iron and oxidized iron with a sixfold oxygen coordination shell similar to that of γ-Fe_2O_3.

Dynamic light scattering (DLS) techniques were used herein to evaluate the size of the water-suspended nanoparticles. It is important to know this measure because the CMNP will most likely be used in liquid medium during the drug-delivery process. Before DLS analysis, the nanoparticles were dispersed in water without addition of surfactant. The suspension was then sonicated overnight. DLS results are presented in Fig. 6, which shows that the diameter of most of the carbon nanoparticles stays in the range of 40-200 nm, with medians at 88 and 160 nm for the benzene- and acetonitrile-synthesized CMNPs, respectively. This is in comparison to the diameter of 40-50 nm that is shown in previous SEM images (Fig. 4), indicating that some small clusters of nanoparticles are formed when CMNP are suspended in water. However, as no surfactant was added to prevent agglomeration, the DLS data are nonetheless very encouraging.

Even though, according to Fig. 6, the average diameter of C/Fe/N CMNPs (acetonitrile-originated) is slightly larger than that of C/Fe CMNP, our subsequent visual inspections showed that the C/Fe/N nanoparticles can actually stay in the non-agglomerated state for several days, whereas the benzene-originated C/Fe nanoparticles quickly settle at the bottom of the suspension within half a day or so. Moreover, when the samples are added into water *without* sonication, the benzene-originated C/Fe CMNPs simply float on the surface and can hardly be dispersed; on the other hand, acetonitrile-originated C/Fe/N nanoparticles almost "dissolve" in water and can be very easily dispersed. This fact indicates that C/Fe/N CMNP

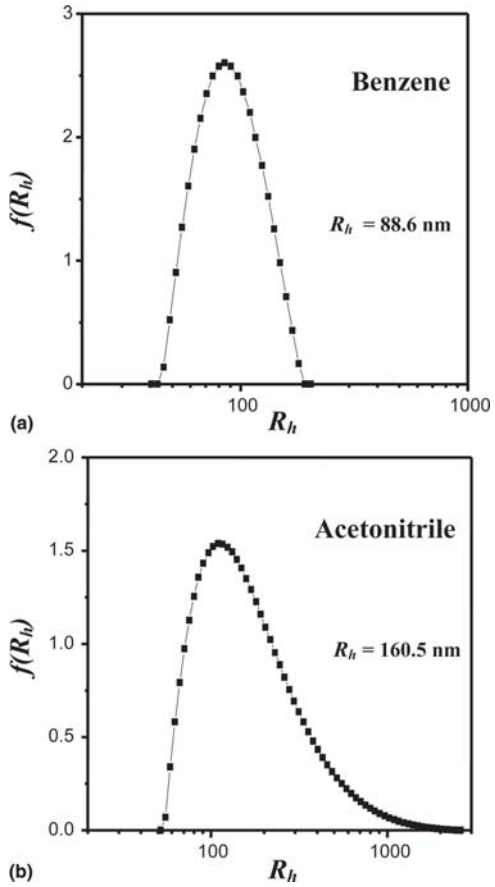

Fig. 6 Dynamic light scattering data from (a) C/Fe (benzene) and (b) C/Fe/N (acetonitrile) nanoparticles; samples dispersed in water by ultrasonication

are much more hydrophilic than the C/Fe nanoparticles. These observations will determine in our future studies how the carbon-based nanoparticles could be used to deliver anticancer agents in the environment of human bodies.

3.2 Formation of CMNP-DOX Conjugates

During immobilization reactions between free doxorubicin and CMNP substrate, the bright orange color of doxorubicin solution was lost within seconds upon being mixed with the CMNP suspension. After the CMNP-DOX conjugate final products were removed, the liquid that remained from the filtration process was almost colorless. These observations suggest that the immobilization reaction was efficient and that the majority of free doxorubicin was consumed during the reaction.

After immobilization reactions, the conjugates were carefully washed many times with three different solvents (i.e., pH 8 buffer, deionized water, and NaCl, as described in Materials and Methods) to remove unreacted doxorubicin. Any unstable Schiff bases should have been hydrolyzed and removed at the same time, and it may not be necessary to use cyanoborohydride at all. In fact, by not reducing the Schiff bases, the equilibrium between them and the free doxorubicin may be exploited to improve the payload-release profile once the CMNP-DOX conjugate is administered and localized in human bodies.

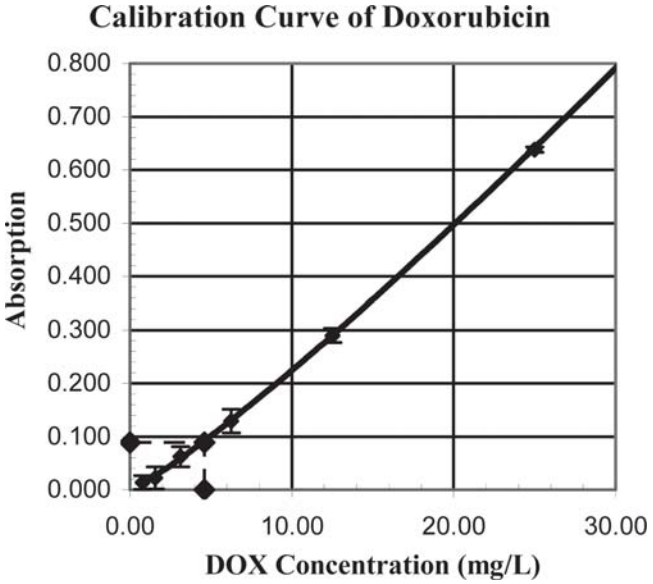

Fig. 7 Spectrophotometer calibration curve for doxorubicin/water solutions, and absorption reading of the water solution left over from washing CMNP-DOX conjugates

As described in Materials and Methods, a spectrophotometer calibration curve (shown in Fig. 7) was established by measuring the absorption of various doxorubicin solutions with known concentrations. After the absorption value of the solution left over from filtration of CMNP-DOX conjugates was obtained with spectrophotometry, the concentration of this solution was determined from the calibration curve. Thus it was calculated that the percentage of untreated doxorubicin is ~4.8%, which is to say that the loading efficiency (the percentage of the drug molecules that have been reacted) is ~95.1%. The percentage of doxorubicin in the CMNP-DOX conjugates was also determined, which is ~10.2%.

3.3 Activity Analysis of CMNP-DOX Conjugates

The addition of DOX or CMNP-DOX to D17 osteosarcoma cells resulted in a dose-dependent inhibition of cell proliferation (Fig. 8). Free CMNP at a concentration that was equivalent to the highest dose of CMNP-DOX had no significant antiproliferative effect. It is theorized that the difference in antiproliferative effect between the free DOX and CMNP-DOX may be as a result of the three-dimensional structure of the magnetic nanoparticle conjugates causing some steric hindrance, limiting the accessibility of some of the DOX molecules to interact with target molecules inside the tumor cells.

4. Conclusions

Carbon-based C/Fe and C/Fe/N magnetic nanoparticles (CMNP) were synthesized in a dense-medium plasma environment. It is shown that the nanoparticles are uniform in size with diameters of 40-50 nm and are magnetic and thermally stable, with iron and iron oxide particles dispersed in a carbon-based host-structure. In particular, the C/Fe/N nanoparticles are fairly hydrophilic and can be easily dispersed in water without apparent agglomeration.

The CMNP were Ar-plasma treated, aminated, and subse-

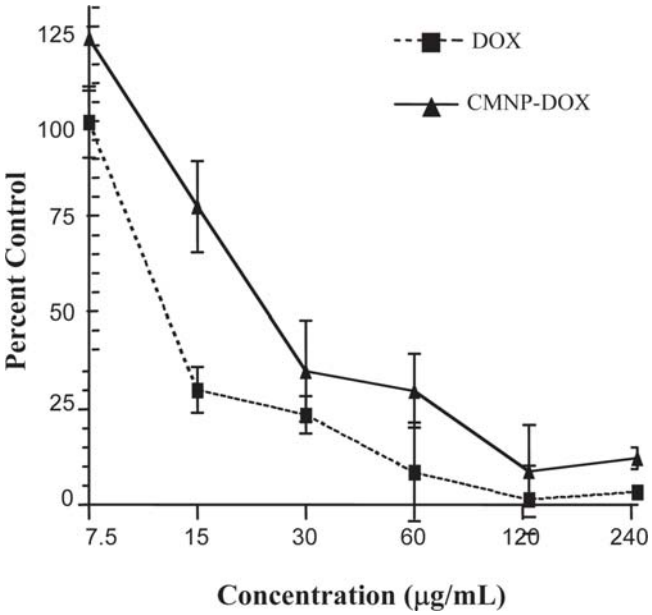

Fig. 8 Anti-proliferative activity of CMNP-DOX against D17 osteosarcoma cells as assessed by MTS assay

quently activated by generating aldehyde groups on the substrate. Free doxorubicin molecules were immobilized onto the surfaces of activated CMNP particles, and the loading efficiency was also determined. The formation of CMNP-DOX conjugates was confirmed by in vitro cytotoxicity assays, which also verified the remaining reactivity of doxorubicin in the CMNP-DOX conjugates. The fact that this CMNP-DOX system is magnetic and retains reactivity of the immobilized drug makes it a potential candidate for targeted drug-delivery applications.

In future work, the immobilization process will be further optimized; the drug conjugates will be tested in vivo on animal subjects (e.g., mice), and these conjugates may one day be used as targeted drug-delivery vehicles and become a viable solution to the usually highly toxic chemotherapies.

Acknowledgments

The authors thank R. Rowell for his help with the ICP-MS and R. Timmons and Z. Hu for the DLS analysis.

References

1. J.H. Fendler, *Nanoparticles and Nanostructured Films: Preparation, Characterization and Applications,* Wiley-VCH Verlag GmbH, Weinheim, Germany, 1998
2. G.C. Hadjipanayis and R.W. Siegel, Ed., *Nanophase Materials, Synthesis, Properties, Applications: Proceedings of the NATO Advanced Study Institute on Nanophase Materials,* Corfu, Greece, June 20-July 2, 1993, NATO ASI Series, Series E, Applied Sciences, Kluwer Academic Publishers, 1994, Vol 260
3. M. de Cuyper and M. Joniau, Binding Characteristics and Thermal Behavior of Cytochrome c Oxidase, Inserted into Phospholipid-Coated, Magnetic Nanoparticles, *Appl. Biochem. Biotechnol.,* 1992, **16,** p 201-210
4. J.H.P. Watson, P.E. Warwick, P.A.B. James, J.M. Charnock, and D.C. Ellwood, Adsorption of Radioactive Metals by Strongly Magnetic Iron Sulfide Nanoparticles Produced by Sulfate-Reducing Bacteria, *Separation Sci. Technol.,* 2001, **36**(12), p 2571-2607
5. P.J. Thomas, P. Saravanan, G.U. Kulkarni, and C.N.R. Rao, Arrays of Magnetic Nanoparticles Capped with Alkylamines, *Pramana J. Phys. [E],* 2002, **58**(2), p 371-383
6. S. Seraphin, J. Jiao, C. Beeli, P.A. Stadelmann, J.-M. Bonard, and A. Chatelain, Encapsulation of Ferromagnetic Metals into Carbon Nanoclusters, *AIP Conf. Proc.,* 1998, p 442, 489-493
7. G.C. Hadjipanayis, Nanostructured Magnetic Materials, *WTEC Workshop Report on R&D Status and Trends in Nanoparticles, Nanostructured Materials, and Nanodevices in the United States*, Proceedings of the May 8-9, 1997, Workshop, WTEC, 1998, p 108-113
8. C.M. Henry, Drug Delivery, *Chem. Eng. News,* 2002, **80**(34), p 39-47
9. Georgia Institute of Technology-Press Release, 2000, Minuscule Magnetic Particles Could Fight Cancer with Fewer Side Effects, http://www.news-info.gatech.edu/news_releases/zhang.html
10. Georgia Institute of Technology-Research News, 2000, Finding the Right Recipe: Researchers Tailor Magnetic Nanoparticles for Medical Treatment & Diagnosis, http://gtresearchnews.gatech.edu/newsrelease/NANOPART2.html
11. A.S. Lübbe, C. Bergemann, W. Huhnt, T. Fricke, H. Riess, J.W. Brock, and D. Huhn, Preclinical Experiences with Magnetic Drug Targeting: Tolerance and Efficacy, *Cancer Res.,* 1996, **56**(20), p 4694-4701
12. S. Rudge, C. Peterson, C. Vessely, J. Koda, S. Stevens, and L. Catterall, Adsorption and Desorption of Chemotherapeutic Drugs from a Magnetically Targeted Carrier (MTC), *J. Controlled Release,* 2001, **74**(1-3), p 335-340
13. M.J. Perez, L. Josephson, and R. Weissleder, Magnetic Nanoparticle Conjugates and Methods of Use, WO 2002098364
14. M. Chastellain, A. Petri, and H. Hofmann, Superparamagnetic Iron Oxide Nanoparticles for Biomedical Applications: A Focus on PVA as a Coating, *Mater. Res. Soc. Symp. Proc.*, 2004, **789,** p 269-272
15. F.S. Denes and R.A. Young, Apparatus for Reaction in Dense-Medium Plasmas, U.S. Patent 5 534 232
16. F.S. Denes, R.A. Young, and Z.Q. Hua, Methods for Reactions in Dense-Medium Plasmas and Products Formed Thereby, U.S. Patent 5 908 539
17. F. Denes, S. Manolache, and N. Hershkowitz, Method and Apparatus for Producing Colloidal Nanoparticles in a Dense Medium Plasma, Patent Application, US2002/0037320A1
18. F. Denes, S. Manolache, Y.C. Ma, V. Shamamian, B. Ravel, and S. Prokes, Dense-Medium Plasma Synthesis of Carbon/Iron-Based Magnetic Nanoparticle System, *J. Appl. Phys.,* 2003, **94**(5), p 3498-3508
19. Y.C. Ma, S. Manolache, M. Sarmadi, F. Denes, Synthesis of Starch Copolymers by Silicon Tetrachloride Plasma-Induced Graft Polymerization, *Starch/Stärke*, 2004, **56,** p 47-57
20. G.T. Hermanson, A.K. Mallia, and P.K. Smith, *Immobilized Affinity Ligand Techniques,* Academic Press, 1992
21. M.J. Barrett, Covalently Bound Biological Substances to Plastic Materials and Use in Radioassay, U.S. Patent 4 001 583
22. G.A. Pietersz, B. Toohey, and I.F. McKenzie, In Vitro and in Vivo Evaluation of Human Tumor Necrosis Factor-Alpha (hTNFalpha) Chemically Conjugated to Monoclonal Antibody, *J. Drug Target.,* 1998, **5**(2), p 109-120
23. H. Kamada, Y. Tsutsumi, Y. Yamamoto, T. Kihira, Y. Kaneda, Y. Mu, H. Kodaira, S.I. Tsunoda, S. Nakagawa, and T. Mayumi, Antitumor Activity of Tumor Necrosis Factor-Alpha Conjugated with Polyvinylpyrrolidone on Solid Tumors in Mice, *Cancer Res.,* 2000, **60**(22), p 6416-6420